ORIGINAL ARTICLE   OPEN

Transcriptional network analysis of peripheral blood leukocyte subsets in multiple sclerosis identifies a pathogenic role for a cytotoxicity-associated gene network in myeloid cells

Margaret A Jordan[1,a] (iD) (Twitter), Melissa M Gresle[2,3,a], Adrian T Gemiarto[1], Dragana Stanley[4], Letitia D Smith[1], Louise Laverick[2], Tim Spelman[5], Jim Stankovich[2], Annie ML Willson[1], Xuyen T Dinh[1,6], Laura Johnson[3], Kylie Robertson[1], Christopher AR Reid[1] (iD), Judith Field[7], Helmut Butzkueven[2,3,a] & Alan G Baxter[1,2,a]

1 Biomedical Sciences & Molecular Biology, CPHMVS, James Cook University, Townsville, QLD, Australia
2 Department of Neuroscience, Central Clinical School, Monash University, Melbourne, VIC, Australia
3 The Department of Medicine, University of Melbourne, Parkville, VIC, Australia
4 Central Queensland University, Rockhampton, QLD, Australia
5 Burnett Institute, Melbourne, VIC, Australia
6 Hai Duong Medical Technical University, Hai Duong, Vietnam
7 CSL Innovation, Parkville, VIC, Australia

Abstract

Multiple sclerosis (MS) is an autoimmune disease of the central nervous system affecting predominantly adults. It is a complex disease associated with both environmental and genetic risk factors. Although over 230 risk single-nucleotide polymorphisms have been associated with MS, all are common human variants. The mechanisms by which they increase the risk of MS, however, remain elusive. We hypothesized that a complex genetic phenotype such as MS could be driven by coordinated expression of genes controlled by transcriptional regulatory networks. We, therefore, constructed a gene coexpression network from microarray expression analyses of five purified peripheral blood leukocyte subsets of 76 patients with relapsing remitting MS and 104 healthy controls. These analyses identified a major network (or module) of expressed genes associated with MS that play key roles in cell-mediated cytotoxicity which was downregulated in monocytes of patients with MS. Manipulation of the module gene expression was achieved *in vitro* through small interfering RNA gene knockdown of identified drivers. In a mouse model, network gene knockdown modulated the autoimmune inflammatory MS model disease—experimental autoimmune encephalomyelitis. This research implicates a cytotoxicity-associated gene network in myeloid cells in the pathogenesis of MS.

INTRODUCTION

Multiple sclerosis (MS) is the most common disabling neurological disease affecting young adults in Western Society, and its incidence is rising.[1] It is a complex disease involving both genetic predisposition (reviewed in Jordan *et al*.[2] and Jordan and Baxter[3]) and environmental insult.[4] A comparison of family-based estimates of heritability with simple models of aggregated genetic risk (generally multiplicative) and a twin study based on a meta-estimation of heritability and environmentability have indicated that approximately 50% of the heritability of MS can be explained by genetics.[5–7] Following the advent of genome-wide association studies (GWAS) in

the past decade, significant strides have been made in identifying MS-associated loci. To date, more than 230 risk loci have been identified in European populations,[8] including 32 variants within the extended major histocompatibility complex; 200 non–major histocompatibility complex genetic loci, distributed throughout the autosome and a single variant on the X chromosome. Many of these associations have been replicated using single-nucleotide polymorphism chip–based genotyping in case–control studies.[5,9–11] The single-nucleotide polymorphisms identified were predominantly associated with genes expressed in immune cell subsets of both the innate and acquired immune systems, consistent with both arms of the immune system contributing to MS pathogenesis. However, none of these variants translate to a protein sequence change, but rather are either intergenic, where the identified gene has been implicated as a result of its proximity to the single-nucleotide polymorphism, or located in introns, although a few are known to have functional consequences on gene expression or splicing (reviewed in Jordan and Baxter[3] and Gresle *et al*[12]). In addition, each affects disease risk only by a small amount.

In an attempt to characterize gene–gene interactions in MS, we drew on the knowledge that the behavior of most complex systems can be modeled by the activity of many components (termed nodes) that interact with each other through pairwise interactions (termed edges) forming a network or graph,[13] in this case, a weighted gene coexpression network analysis (WGCNA). A gene coexpression network is an undirected graph, where each node corresponds to a transcript, and a pair of nodes is connected by an edge if there is a significant coexpression relationship between them, but the correlated expression itself does not define the nature of the relationship. Genes encoding proteins that participate in the same pathway or are part of the same protein complex may be expressed in patterns that are correlated in a diverse range of conditions, producing modules and networks that are conserved, even across evolutionarily diverse organisms.[14] In a WGCNA, the stronger the correlation of expression between a pair of transcripts, the shorter the edge between the nodes representing them.[15] Taking this approach, together with our knowledge that both innate and adaptive immune cell subsets were important, we recruited 76 people with relapsing remitting MS (pwRRMS) and 104 age- and sex-matched healthy, unrelated individuals [i.e. healthy controls (HCs)]. We then constructed a gene coexpression network, comparing gene expression between MS-affected and unaffected individuals, on five sorted leukocyte populations, to help elucidate the underlying mechanisms of disease.

RESULTS

Weighted gene coexpression network construction

A WGCNA was constructed based on 688 microarrays surveying genome-wide transcription of all five sorted leukocyte populations, from untreated pwRRMS and HCs. Sources of variation encompassed in the resulting model included differences in gene expression related to disease phenotype and those dependent on allelic, cell lineage–specific and idiosyncratic factors. Principal component analysis mapping indicated that the variability was strongly correlated with leukocyte subsets, with samples generally grouping according to subsets rather than by differences between diseased and HC samples. Variability of transcripts across all arrays was ranked by standard deviation[16] and the 19 659 most variable transcripts were used for network construction. Application of the WGCNA algorithm in R[17] (R Foundation, Vienna, Austria) generated a WGCN of 5762 nodes and 198 937 edges assigned to 16 distinct coexpressed modules (Figure 1a).

Disease-associated transcriptional differences

The cohorts of patients and controls whose samples were used to identify transcripts differentially expressed between the two groups were primarily composed of the samples used for network construction with the following exceptions: nine individuals (seven patients and three HCs) were removed because of a subsequent primary progressive MS or secondary progressive MS diagnosis, administration of disease-modifying therapeutics, incomplete patient data availability or that they were control cases subsequently identified as being related to a person with MS. Individual samples with purities lower than 95% were also removed from the analyses. Overall, there were 65 patients with RRMS and 97 HCs meeting all criteria. The demographic of study participants and sample numbers per cell type are listed in Table 1.

To identify expression modules associated with MS, a Student's *t*-test *P*-value was calculated for each transcript in each cell type, testing the null hypothesis that expression levels did not differ between patients and HCs. These *P*-values were mapped onto the network and visualized in Cytoscape 3.10 (Institute for system biology, Seattle, USA)[18] using a heat map to represent the strength of disease association. Highly differentially expressed (HDE) transcripts were defined as those with the Student's *t*-test *P*-value below a Bonferroni corrected significance threshold of 1.5×10^{-6}. The resulting networks for each cell type are illustrated (Figure 1b, monocytes; c, B cells; d, natural killer (NK) cells; e, CD4$^+$
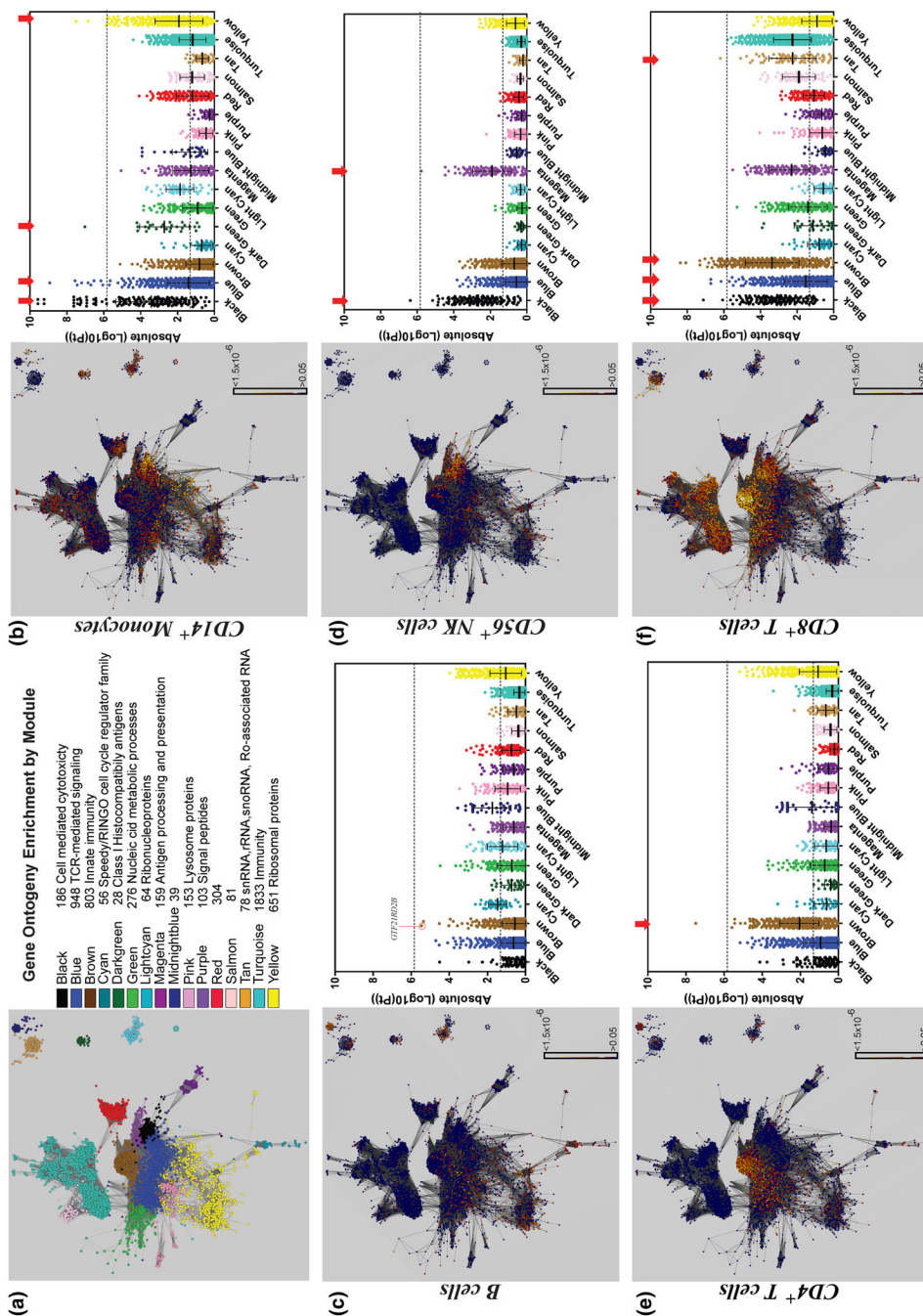
Figure 1. Weighted gene coexpression network. A WGCN constructed, using Combat R and Cytoscape 3.10, on microarrays surveying genome-wide transcription of five sorted leukocyte populations from peripheral blood of pwMS and HCs. **(a)** Network containing 5762 nodes and 198 937 edges assigned to 16 significantly coexpressed modules, with key illustrating module names and associated GOE. **(b–f)** The Student's *t*-test was used to assign pairwise *P*-values to pair-wise expression values from patients and HCs to each transcript, which were illustrated by heat maps for each cell type and graph mapped onto the network illustrated in a: **(b)** monocytes; **(c)** B cells; **(d)** NK cells; **(e)** CD4$^+$ T cells; **(f)** CD8$^+$ T cells. (dark blue represents an uncorrected *P*-value > 0.05; white, an uncorrected *P*-value < 1.5×10^{-6}, a threshold determined by a conservative Bonferroni correction). Alongside each are box plots illustrating for each module the distribution of *t*-test–derived *P*-values (expressed as the absolute Log$_{10}$ of the value) derived by comparing expression levels of each transcript of patients with MS and HCs. The horizontal dashed line indicates the uncorrected *P*-value threshold determined by Bonferroni correction, above which are the HDE transcripts. Data are derived from 76 untreated patients with RRMS and 104 HCs. GOE, gene ontogeny enrichment; HC, healthy control; HDE, highly differently expressed; MS, multiple sclerosis; NK, natural killer; pt, patients; pwMS, people with MS; RRMS, relapsing-remitting multiple sclerosis; rRNA, ribosomal RNA; snRNA, small nuclear RNA; snoRNA, small nucleolar RNA; TCR, T-cell receptor; WGCN, weighted gene coexpression network.

Table 1. Inclusion/exclusion criteria, study data composition and demography of study participants.

	People with multiple sclerosis (RRMS)	Healthy volunteers (healthy controls)
A. Inclusion/exclusion criteria	Definite RRMS according to the McDonald criteria	—
	Aged between and inclusive of 18–65 years of age	Aged between and inclusive of 18–65 years of age
	Not currently on immunomodulating therapy for MS, or none within the last month	—
	No other concurrent autoimmune disease	No personal history of neurological disease or autoimmune disease
	No medical contraindications to MRI scanning, including gadolinium allergy, renal impairment, cardiac pacemakers or claustrophobia	Has no known relative with MS
B. Composition of study data collection	Demographic information	Demographic information
	Age	Age
	Gender	Gender
	Date of first MS attack	—
	Time of last MS relapse	—
	Date of last treatment with intravenous methylprednisolone for MS attack	—
	Number of relapses in the last 2 years	—
	Quantitated neurological evaluation expressed as Kurtzke Functional Systems scores, to calculate the Expanded Disability Status Score	—
	White blood cells (obtained from one venous blood sample, approximately 100 ml)	White blood cells (obtained from one venous blood sample, approximately 100 ml)
	Cerebral MRI scan (with gadolinium contrast–enhanced sequences and diffusion-weighted sequences)	—
C. Demography of study participants		
Total participants	76	104
Average age (range), years	37.05 (20–63.4)	38.3 (21.3–64)
Disease duration (range), years	8.64 (4.8 months to 32 years)	—
Expanded Disability Status Score (range)	1.8 (0–6)	—
D. Cell type (> 95% pure), n (male, female; male:female)		
CD56$^+$ NK cells	50 (12,38; 1:3.2)	91 (31,60; 1:1.9)
CD14$^+$ monocytes	65 (18,47; 1:2.6)	97 (34,63; 1:1.9)
B cells	32 (5,27; 1:5)	85 (31,54; 1:1.7)
CD4 T cells	37 (9,28; 1:3)	81 (27,54; 1:2)
CD8 T cells	49 (12,37; 1:3)	86 (32,54; 1:1.7)

F, female; M, male; MRI, magnetic resonance imaging; NK, natural killer; RRMS, relapsing remitting multiple sclerosis.

T cells; f, CD8$^+$ T cells) alongside their absolute log P-value for the genes in each module. Gene Ontology (GO) enrichment features, scores and significantly differentially regulated genes per cell type are represented in Supplementary table 1.

Across all modules and cell types, the BLACK module in monocytes contained the greatest proportion of transcripts that were HDE between pwRRMS and HCs (12 of the 22 HDE genes in monocytes ($P < 10^{-34}$, χ^2 test; Figures 1 and 2)), suggesting an important association with MS. Remarkably, all 12 of these were expressed at lower levels in pwRRMS than in healthy controls.

The BLACK module and cytotoxicity

The BLACK module is a tightly regulated transcriptional module consisting of 186 genes (Figure 2a;
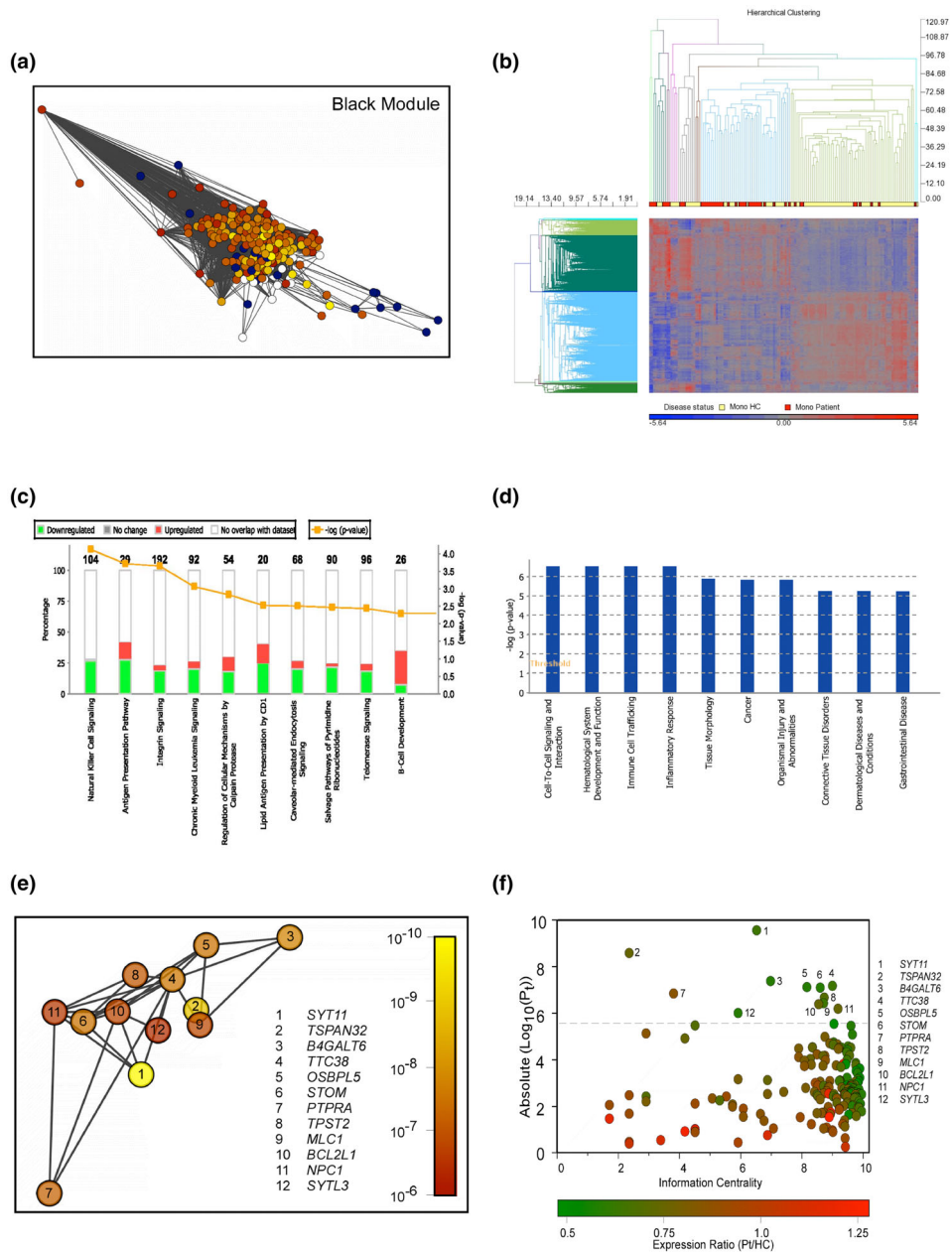
Figure 2. BLACK module gene expression in monocytes. **(a)** Graph of the BLACK module isolated from the rest of the network, with heat map applied (dark blue represents an uncorrected *P*-value > 0.05; white, an uncorrected *P*-value < 1.5×10^{-6}, a threshold determined by a conservative Bonferroni correction). **(b)** Heat map and hierarchical clustering of monocyte differential expression between patients (yellow) and HCs (red) generally grouped patients with RRMS as distinct from HCs in relative gene expression. **(c)** The top 10 canonical pathways identified by Ingenuity Pathways Analysis (IPA; Ingenuity Systems Inc) for the BLACK module genes expressed in monocytes. Green, downregulated; red, upregulated; and gray, no change. **(d)** The top 10 enriched pathways identified for the monocyte differential expression analysis (Partek Flow analysis of variance (Partek SG, Singapore). **(e)** Graph of the HDE transcripts from the BLACK module with a separate heat map illustrating *t*-test–derived *P*-values derived by comparing expression levels of each transcript from monocytes of patients with MS and HCs. Sliding scale representing the least HDE transcripts with *P*-value of 10^{-6} to most HDE in light yellow with *P*-value of 10^{-10}, with the threshold determined by a conservative Bonferroni correction. The key identifies the gene symbols associated with each transcript. **(f)** Dot plot of all transcripts in the BLACK module for each transcript showing the network information score (*x*-axis), absolute $\log_{10}$ of the *P*-value (*y*-axis) and differential expression (expression ratio patients/HCs; sliding scale: green represents the most downregulated and red the most upregulated). HC, healthy control; HDE, highly differentially expressed; MS, multiple sclerosis; RRMS, relapsing-remitting multiple sclerosis.

Supplementary table 1), many of which encode components of the type 1 T helper/cytotoxic pathway. Coregulated genes within this module were *PRF1* (perforin); *IFNG* [interferon gamma (IFNγ)]; *FASLG* (Fas ligand); *PIK3R3* (phosphatidylinositol 3-kinase regulatory subunit gamma); *SH2D1B* [SH2 domain-containing protein 1B, a cytoplasmic adapter regulating receptors of the signaling lymphocytic activation molecule (SLAM) family]; *NCR1* (natural cytotoxicity triggering receptor 1); *NKG7* (natural killer cell granule protein 7); *CD8A* (CD8 antigen); interleukin receptors *IL12RB2* and *IL18RAP*; *DTHD1* (death domain containing 1); *CD160/NK1* [encodes a ligand for HVEM (TNFRSF14)]; *XCL2* (encodes a protein that induces chemotaxis of cells expressing the chemokine receptor XCR1); *PDGDR* (platelet-derived growth factor receptor); *GNLY* (granulysin); 3 granzymes and 20 KIR (killer-cell immunoglobulin-like receptor) genes and two master regulators already identified as MS-susceptibility genes by GWAS, the transcription factor *EOMES* [eomesodermin (also known as T-box brain 2)] and its highly homologous *TBX21* (T-box expressed in T cells, encodes T-bet) gene. The list of transcripts within the BLACK module was submitted to The Database for Annotation, Visualization and Integrated Discovery (DAVID) Bioinformatics Resources 6.7[19] for analysis of functional annotation clustering. The top annotation cluster (Enrichment Score 10.65) contained the following immune processes: NK cell–mediated cytotoxicity (hsa04650), graft-versus-host disease (hsa05332) and antigen processing and presentation (hsa04612).

The BLACK module and MS

The BLACK module of genes was downregulated in the monocytes of pwRRMS compared with HCs. Hierarchical clustering generally grouped patients with RRMS as distinct from HCs in relative gene expression (Figure 2b), and the antigen processing and presentation and NK cell–mediated cytotoxicity pathways were shown as the top two enrichment pathways when analyzed in Partek Pathway Analysis, with enrichment scores of 17.3581 (enrichment *P*-value 2.89 × 10^{-8}) and 14.1518 (*P*-value = 7.14 × 10^{-7}), respectively. The full list of transcripts with FDR ($P < 0.005$) was submitted to ingenuity pathway analysis with a filter to exclude endogenous chemicals and a consideration of only relationships with a confidence level of "experimentally observed". The top canonical pathways (Figure 2c) were NK cell signaling [$P = 7.31 × 10^{-5}$; overlap 27.9% (29/104)], antigen presentation pathway [$P = 1.87 × 10^{-4}$; overlap 41.4% (12/29)], integrin signaling [$P = 2.18 × 10^{-4}$; overlap 22.9% (44/192)],

chronic myeloid leukemia signaling [$P = 8.5 × 10^{-4}$; overlap 26.1% (24/92)] and regulation of cellular mechanisms by calpain protease [$P = 1.44 × 10^{-4}$; overlap 29.6% (16/54)]. Given that gene set enrichment focuses on genes that show considerable differences in expression level between the conditions, any subtle changes in expression levels that may still result in profound biological consequences could have been missed, therefore we also applied a pathway analysis of variance (Partek Flow, (Partek SG, Singapore)) which compares the path coefficients of the two groups to give us additional biological insight. The top 10 enriched pathways were mostly related to cell signaling, interaction and trafficking (Figure 2d; Supplementary table 2).

A description of the 12 HDE monocyte transcripts of the BLACK module, *SYT11*, *TSPAN32*, *STOM*, *B4GALT6*, *OSBPL5*, *TTC38*, *PTPRA*, *TPST2*, *BCL2L1*, *MLC1**, *NPC1* and *SYTL3**, is given in Table 2 (* indicates previously associated MS risk variants) and their correlations (edges) with each other are illustrated in Figure 2e,f and Supplementary figure 2, all of which were significantly downregulated in monocytes of patients with RRMS. While several members of the NK cell–mediated cytotoxicity pathway were downregulated in monocytes of patients with MS, the genes with the largest negative fold change were *KLRC2*, *KLRC4-KLRK1*, *KLRC3*, *SH2D1B*, *KLRC4*, *KLRF1**, *DTHD1*, *CD160/NK1*, *KLRC1*, *IL18RAP*, *XCL2* and *PTGDR*, indicating that killer cell lectin-like receptor subfamily C members were predominantly implicated.

Manipulation of BLACK module genes

As all genes within a module are highly connected, we hypothesized that a hub(s) (highly connected node(s)) could be identified with the ability to modulate BLACK module expression in its entirety. Current-flow closeness centrality is a variant of closeness centrality based on effective resistance between nodes in a network. This metric is also known as information centrality. As network theory predicts that nodes with high information centrality will affect a larger proportion of transcripts, we examined the information centrality of the HDE genes and other members of the BLACK module in monocytes (Figure 2f), to determine the best candidate transcripts by degree, eigenvector, betweenness and closeness centrality to rank the gene–disease associations. Of the HDE transcripts, all were downregulated in monocytes of patients with MS, with *TTC38*, *OSBPL5*, *STOM*, *PTPRA*, *TPST2*, *MLC1*, *BCL2L1* and *NPC1* showing the highest control over the flow of information within the network (represented in Figure 2f). The two transcription factors, *EOMES* and *TBX21*, previously identified as

Table 2. List of highly differentially expressed genes identified in the Black module in the Monocyte analysis.

	Affy ID	P-value (ANOVA)	FC in RRMS	Gene ID	Description (http://www.ncbi.nlm.nih.gov/)	Protein Functions/role in cell (ingenuity pathway analysis gene view)	Regulates/Binds:
1	7906061	4.34×10^{-10}	−1.5	SYT11	Synaptotagmin XI	Calcium-dependent phospholipid binding, calcium ion binding, protein binding, transporter	Regulates neurotransmitter, SYT11; binds UBC, SGTA, PARK2, APPBP2, SYNCRIP, SND1, PDIA6, VTI1A, FMR1, RGD1560475, AGO2, ATP13A2, CSNK1A1 and MYLK
2	7937782	8.29×10^{-10}	−1.3	TSPAN32	tetraspanin_LEL, Tetraspanin family	Proliferation, organization, activation and aggregation	Regulates IL-2
3	8022747	6.16×10^{-8}	−1.5	B4GALT6	UDP-Gal:betaGlcNAc beta 1,4-galactosyltransferase, polypeptide 6	Enzyme, galactosyltransferase, UDP-galactose-glucosylceramide beta-1, 4-galactosyltransferase	Regulates glycosphingolipid, sphingolipid, Erk1/2, Ras, lactosylceramide (LacCer), 150 GFAP; binds ST3GAL5, A4GALT, ZFP36. Involved in lipid biosynthesis
4	8073842	2.61×10^{-8}	−1.5	TTC38	Tetratricopeptide repeat domain 38	Unknown	Binds UBC, TK1, PFDN1, HNF4A
5	7945831	3.34×10^{-8}	−1.5	OSBPL5	Oxysterol-binding protein-like 5	Cholesterol binding	Binds UBC, GATB, NPC1, APP, HGS, ABL1
6	8163896	2.29×10^{-7}	−1.5	STOM	Stomatin	Role in cell: morphology	Binds UBC, SLC2A1, ASIC3, RAPGEF2, DVL3, FBXO6, RUVBL1, RPL13A, ADRB2, RUVBL2, SVIL, VCAM1, FN1, ITGA4, FMNL1
7	8060539	1.04×10^{-7}	−1.2	PTPRA	Protein tyrosine phosphatase, receptor type, A	Binding, transformation, migration, activation, abnormal morphology, formation, morphology, differentiation, assembly, growth	Regulates SRC, FYN, PTK2, IRS1, PTPRA, ITPR1, PAG1, MAPK1, Erk, PDGFRB, MS4A2, INSR, LYN, BCAR1 and GRIN2B; binds GRB2, PTPRA, SRC, UBC, BCAR1, HSPB1, Contactin, PDGFRB, INSR, ITGAV, CD63, PTPRN2, PTPRF, PTPRM and CALM1
8	8075106	3.89×10^{-7}	−1.3	TPST2	Tyrosylprotein sulfotransferase 2	Fusion, motility, expression in morphology	Regulates Adam3, Adam6a/Adam6b, TSHR
9	8076894	1.94×10^{-7}	−1.4	MLC1	Megalencephalic leukoencephalopathy with subcortical cysts 1	MLC1 is a transmembrane protein exclusively expressed in the brain. It is abundant in astrocyte–astrocyte junctions and is involved in regulation of cellular water balance	Binds KCNJ10, DTNA, ATP1B1, UBC, DISC1, TRPV4, CAV2, KDM1A, CAV1, SNTA1, DTNB, PRMT6, syntrophin, MYH3, TUBA1A

(Continued)

Table 2. Continued.

	Affy ID	P-value (ANOVA)	FC in RRMS	Gene ID	Description (http://www.ncbi.nlm.nih.gov/)	Protein Functions/role in cell (ingenuity pathway analysis gene view)	Regulates/Binds:
10	8065569	4.97×10^{-7}	−1.3	BCL2L1	BCL2-like 1	Role in cell apoptosis, survival, cell death, proliferation, transmembrane potential, growth, cell cycle progression, quantity, autophagy, cell viability	Regulates CYCS, CASP3, CASP9, cytochrome C, BAX, BCL2L11, CASP8, Caspase, BAK1, DIABLO, BID, P38 MAPK, AIFM1, VDAC1, BECN1; binds BAD, BAX, BCL2L11, BAK1, BID, BBC3, BECN1, BIK, TP53, BCL2, UBC, APAF1, VDAC1, HRK, PMAIP1
11	8022531	8.94×10^{-7}	−1.3	NPC1	Niemann–Pick disease, type C1	Role in cell: accumulation, cell death, quantity, entrance, autophagy by, macro-autophagy, trafficking, apoptosis, expression, fusion	Regulates cholesterol, ABCA1, SREBF2, LDLR, sphingosine-1-phosphate, D-sphingosine, ganglioside GM2, ganglioside GM3, Ca^{2+}, CTSK, ABCG1, MYLIP, Hmg CoA Synthase, CTSD, asialo GM2 ganglioside; binds UBC, STUB1, HSPA8, calnexin, Hsc70, Hsp70, LGR4, FBXO6, Hsp90, UNC93B1, TMEM173, NPC2, OSBPL5, VPS4A, LRP6
12	8123080	2.68×10^{-6}	−1.4	SYTL3	Synaptotagmin-like 3	Calcium-dependent phospholipid binding, role in cell: exocytosis	Regulates NPY; binds RAB27A, STXBP1, DLG4, KLC1, UBC, RAB27B, RAB10, NRXN1

FC, fold change; IL, interleukin; RRMS, relapsing remitting multiple sclerosis.

MS-susceptibility genes in GWAS, were both downregulated in monocytes of patients with MS and were identified here as highly information central. *EOMES* alone was shown to be the nearest neighbor of 133 of 186 transcripts in the BLACK module and had a total of 282 nearest neighbors, while *TBX21* alone was the nearest neighbor of 103/186 BLACK module transcripts and had a total of 135 nearest neighbors. We therefore undertook to modulate the expression of the entire BLACK module as an integrated unit in human monocytes and in mice.

In vitro manipulation of BLACK module genes

Gene expression effects of lentiviral knockdown (KD) on other HDE candidates and the other BLACK module genes were examined. Genes were silenced, individually or in combination, *in vitro* in a human monocytic cell line, THP-1(ATCC#TI-B202), using small interfering RNA (siRNA, Thermo Fisher Scientific, USA) and Lipofectamine RNAiMAX (Thermo Fisher Scientific, USA), and then visualized by quantitative PCR (Figure 3) or gene expression microarray. In general, approximately 20–60% of the candidate genes' messenger RNA were silenced as measured 48 h after transfection and resulted in downregulation of other BLACK module transcripts with minimum effect on two statistical controls, *HINT1* (not included in the network) and *MPG* (a member of the Turquoise module). In at least two independent experiments, silencing of *BCL2L1* was shown to be the most effective, with a 60% decrease in *BCL2L1* messenger RNA compared with control siRNA 48 h after transfection. Despite this, KDs of *TPST2, SYTL3, TBX21* and *EOMES* were shown to be most efficient in decreasing the expression of other HDE genes (Figure 3) and the BLACK module genes as a whole. Silencing of EOMES resulted in the downregulation of *SYT11* (0.34 ± 0.07), *OSBPL5* (0.76 ± 0.12), *B4GALT6* (0.68 ± 0.14), *STOM* (0.56 ± 0.06), *BCL2L1* (0.75 ± 0.03) and *NPC1* (0.79 ± 0.11), while silencing of *TBX21* was accompanied by simultaneous downregulation of *SYT11* (0.13 ± 0.07), *OSBPL5* (0.72 ± 0.14) and *MLC1* (0.76 ± 0.06). Having confirmed the close association of our HDE candidates, we then tested whether we could manipulate the BLACK module, as a unit, through modulation of expression of a single or a few genes. For this, we selected three candidate genes, *TPST2, BCL2L1* and *EOMES*, based on their silencing efficiency (~35–60% downregulation of the respective transcripts) and lack of evidence of upstream regulators. We analyzed the effect of *in vitro* downregulation of each gene in THP-1 cells on the BLACK module genes via microarray analyses. Our findings indicated that the

BLACK module could be modulated by targeting a subset of the module's genes. Single-gene KD resulted in a decrease in expression between 20% and 43% of the BLACK module genes (Figure 3). Double-gene KDs resulted in a similar outcome.

Experimental autoimmune encephalomyelitis in targeted knockout mice

EOMES and *Tbx21*/*Tbet* gene (together referred to as *ET*) are transcription factors controlling T- and NK-cell differentiation[20,21] and have previously been reported to bridge innate and adaptive immunity, as they are expressed in DCs, NK cells, NKT cells and innate lymphoid cells, as well as CD4^{+} and CD8^{+} T effector cells, B cells, γδ T cells and a subset of regulatory T cells.[20] In 2014, Parnell and colleagues[22] implicated a role for ET in MS, with low molecular phenotype being identified in whole blood of untreated patients with MS and those with clinically isolated syndrome. In 2016, they showed that this was accompanied by CD56^{+} cell dysregulation and that expression could be normalized to healthy control levels with the immunomodulatory therapy natalizumab.[23] We therefore used Cre-Lox technology to specifically target *Eomes* or *Tbx21* KD in either the myeloid lineage or NK cells. This approach was used to investigate whether either cell population, through their ability to regulate the BLACK module, could affect disease severity. Following MOG$_{35-55}$-induced experimental autoimmune encephalomyelitis (EAE) induction, mice were scored for disease-modifying effects of targeted reduction of EOMES or TBX21 for 30 days.

Comparison of EOMES KD in myeloid cells with wild-type (WT) control mice (Figure 4a, b, e, f), showed significantly earlier disease onset in the female mutant strain (9.8 ± 1.1 *vs* 12.4 ± 0.4; *P* < 0.05, Mann–Whitney *U*-test), but with significantly milder signs of disease (maximum clinical score 2.8 ± 0.1 *vs* 3.1 ± 0.1; *P* < 0.05, Mann–Whitney *U*-test) and only half of them reaching a maximum clinical score of 3. By contrast, all control mice developed disease with a clinical score of 3 or higher. Differences in severity of the disease course as analyzed by the evaluation of the area under the curve showed significantly milder disease in the KD strain (31.6 ± 3.8 *vs* 41.6 ± 1.4; *P* < 0.05, Mann–Whitney *U*-test). No differences in time to disease onset were observed in male mice (11.7 ± 0.4 *vs* 10.7 ± 0.6, *P* = 0.05, Mann–Whitney *U*-test) nor in maximum clinical score, but there was striking disease recovery in male mutant mice within a few days after the disease peaked at a score of 3, which contributed significantly to the reduced area under the curve and cumulative EAE score (32.5 ± 3.0 *vs* 45.3 ± 2.9; *P* < 0.05, Mann–
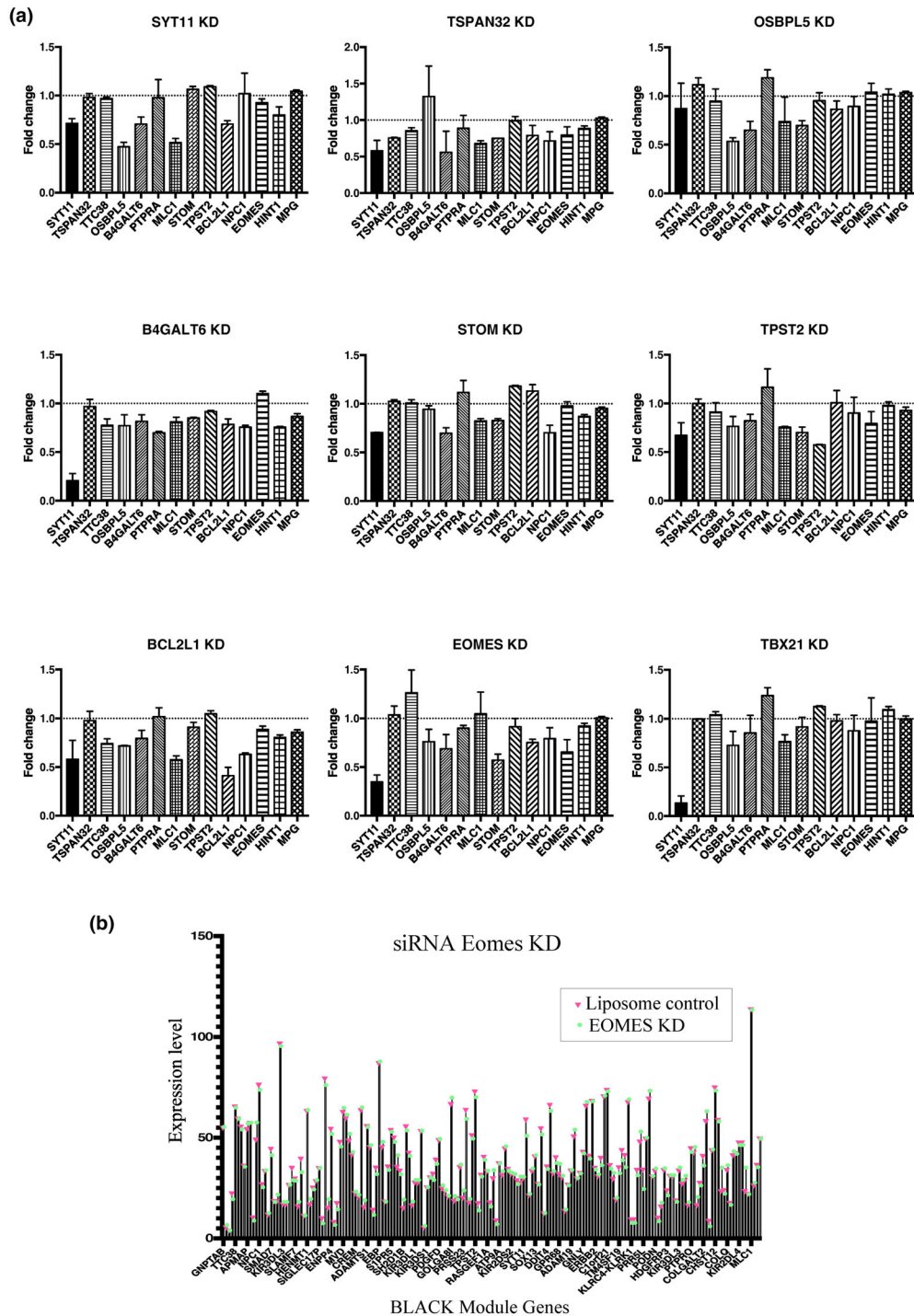
Figure 3. *In vitro* knockdown of HDE candidate genes. Changes in mRNA expression of HDE BLACK module genes in THP-1 cells 48 h after siRNA delivery. THP-1 cells were transfected for 48 h with 65 nM of Silencer Select siRNA for each candidate gene. Data are represented as mean fold change of gene expression ± standard error of the mean of at least two independent experiments (normalized to GAPDH). **(a)** Genes with < 1.0-fold change value indicates downregulation, genes with > 1.0-fold change value indicates upregulation as determined by quantitative PCR for HDE candidates and **(b)** by microarray across all 181 BLACK module genes as represented here for *EOMES* silencing in THP-1 cells. GAPDH, glyceraldehyde 3-phosphate dehydrogenase; HDE, highly differently expressed; KD, knockdown; mRNA, messenger RNA; siRNA, small interfering RNA.
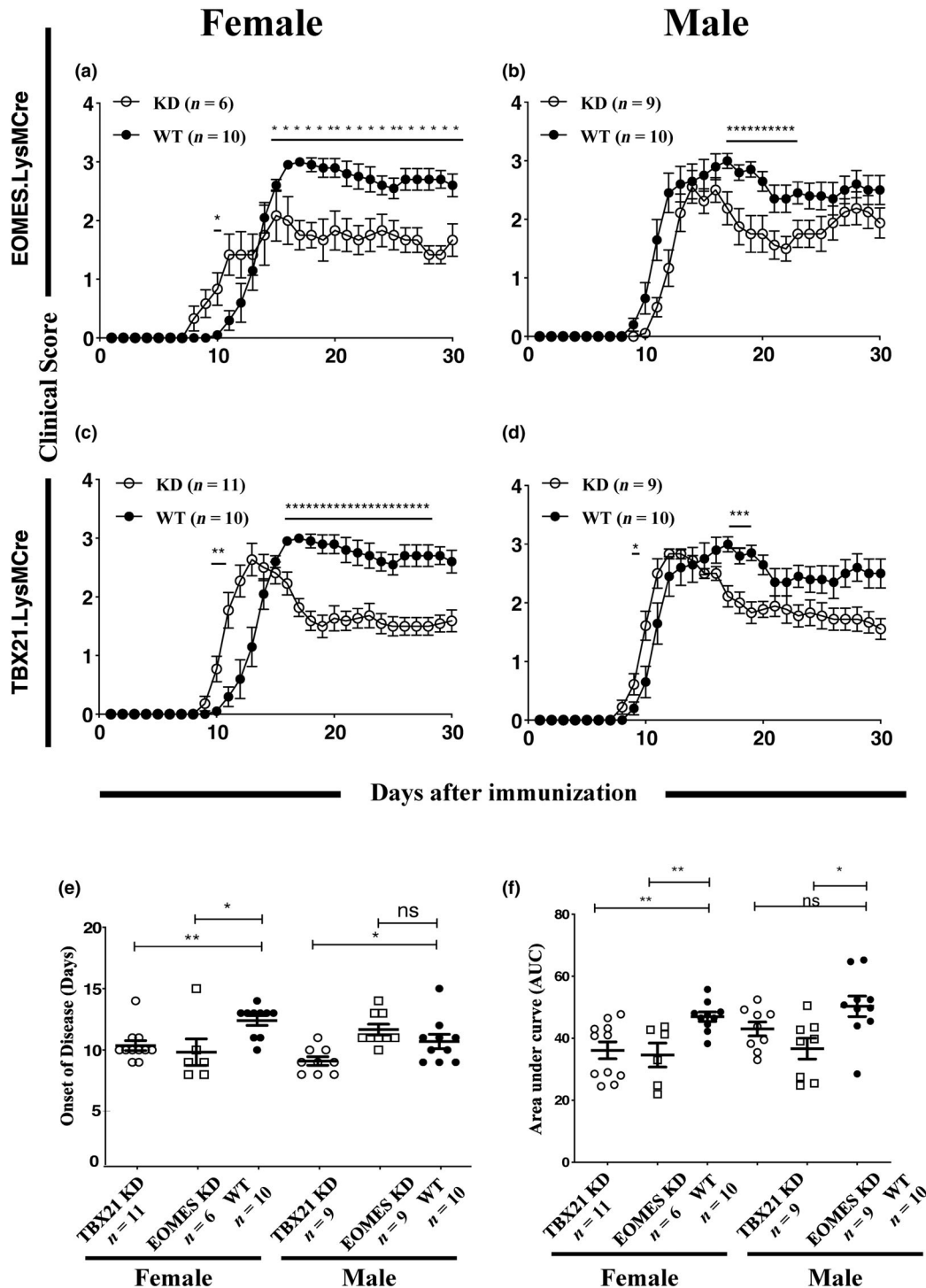
Figure 4. EAE following *in vivo* gene knockdown in monocytes. EAE disease course in female **(a, c)** and male **(b, d)** B6.*Eomes.LysMCre* + and B6.*Tbx21.LysMCre* + mice (KD; open circles) compared with age-matched B6 wild-type mice (closed circles) from two independent experiments. Each data point in **(a–d)** represents the mean ± SEM of at least six animals per group. A statistical difference in the clinical score between the controls and the KD mice at each point are indicated by * (*P < 0.05, uncorrected Mann-Whitney *U*-test). The onset of EAE is significantly earlier in *Eomes* and *Tbx21*– KD females **(e)** and the disease severity is significantly lower in both sexes for both knockdowns **(f)** compared with control mice. Data are presented as mean ± standard error of the mean. Mann–Whitney *U*-test; *P < 0.01, **P < 0.001. n = 6–11. EAE, MOG$_{35–55}$-induced experimental autoimmune encephalomyelitis; KD, gene knockdown mice; ns, not significant; WT, wild type.

Whitney *U*-test). Both male and female mice with *Tbx21* myeloid cell–targeted deletion developed EAE symptoms significantly earlier than WT mice (Figure 4c–f; 9.1 ± 0.4 *vs* 10.7 ± 0.6 for males; $P < 0.01$, Mann–Whitney *U*-test and 10.4 ± 0.4 *vs* 12.4 ± 0.4 for female mice; $P < 0.001$, Mann–Whitney *U*-test); however, the disease severity was significantly lower in the KD mice, of both sexes, from day 16 onward ($P < 0.05$, Mann–Whitney *U*-test; Figure 4f; area under the curve 39.7 ± 1.9 *vs* 45.3 ± 2.9 and 33.0 ± 2.5 *vs* 41.6 ± 1.4; $P < 0.05$, Mann–Whitney *U*-test). The mutant mice showed marked recovery during the chronic phase in both EOMES and TBX21 KD, while the control group maintained severe disease throughout this phase. EAE disease course comparisons between Cre^+ and Cre^- littermates showed the same trend to earlier onset and disease recovery, particularly in female mutant mice, although this was a more subtle but reproducible effect (male: day of onset 12.2 ± 0.5 *vs* 11.9 ± 0.4; female: 11.9 ± 0.5 *vs* 12.8 ± 0.6 days after induction; $P > 0.05$, Mann–Whitney *U*-test).

TBX21 KD targeted to NK cells showed no differences in time to onset or disease course compared with littermates of either sex (Figure 5a–d). Although our data are limited by the lack of assessment in female mice of EOMES KD targeted to NK cells (as a result of disproportionately fewer numbers of females being born from mating to produce the KD mice), experiments in male mice indicated that there was no change in time to onset, but that slight, yet significant, worsening of disease course without recovery was observed (Figure 5e, f) that may possibly be attributed to the decrease in NK cells.

DISCUSSION

To date, only limited attempts to apply network theory to MS have been made. Most of these have been candidate pathway analyses based on the International Multiple Sclerosis Genetics Consortium[8] genetic association data set where protein-coding regions were implicated because of their proximity to known risk single-nucleotide polymorphisms. These lists were then submitted to interaction databases via VisANT to identify common "interactors" or "first neighbors". In general, these studies have found that the protein products of GWAS-implicated genes are more likely to interact physically and to belong to the same or related pathways. They have implicated networks including key T-cell cytokines, tumor necrosis factor family signaling and cell adhesion molecules. Nickles and colleagues[24] studied the longitudinal gene expression profiles of whole-blood RNA from a cohort of 195 patients with MS and 66 HCs, identifying 62 transcripts that were upregulated in patients. This gene list was mapped onto the Human Protein Reference Database's protein–protein interaction network to identify 52 significantly associated modules, one of which was associated with immune cell and cell cycle–related pathways. Menon and colleagues[25] also compared the transcripts of whole blood between patients with RRMS and HCs, where they identified 207 genes as differentially expressed between 12 RRMS females compared with 9 HCs, and 72 differentially expressed genes between 9 male patients with RRMS and 12 HCs. This approach identified a hierarchy of interactors heavily associated with the products of differentially expressed genes (or the genes themselves), including *TP53*, *IKBKG*, *RELA* and *SP1*.

Until now, three gene coexpression network analyses of MS have been performed. The first was limited in scope by the use of quantitative PCR to quantify only 20 transcripts from whole blood. A network was constructed by Bayesian analysis and was restricted to associations described in the Ingenuity Pathways Knowledge Base.[26] This approach identified the Notch signaling pathway as implicated in MS. Consistent with this conclusion, the administration of a Jagged1 agonist peptide to mice reduced the severity of EAE in this mouse model of central nervous system autoimmunity.[27] The second study used microarrays to survey genome-wide transcription in whole blood from 99 untreated patients with MS (36 RRMS, 43 primary progressive MS and 20 secondary progressive MS) and 45 HCs. One of two approaches applied to the data set was to search pairwise for groups of genes differentially coexpressed between patients and controls. Of these, groups of genes with high centrality were then examined for over-represented sequence motifs to identify their corresponding transcription factor. Some of the transcription factors identified are known to be involved in T-cell or oligodendrocyte development, including the EGR/KROX family, ATF2, YY1, E2F-1/DP-1 and E2F-4/DP-2 heterodimers, SOX5 and CREB and ATF families.[28] In the third study, Creanza and colleagues[29] reanalyzed 595 messenger RNA arrays from publicly available whole blood data sets to study changes in gene coexpression networks in MS and in response to interferon beta treatment. They showed reduced connectivity of MS networks in untreated individuals, which was increased following treatment. In addition, they reported that some genes, previously proposed as candidates by GWAS, showed no evidence of differential expression but were, however, associated with functional changes of other connected genes. These studies all relied on the mixed and variable leukocyte populations of peripheral blood and tended to restrict conclusions to relationships described in interaction databases. As a result, they were
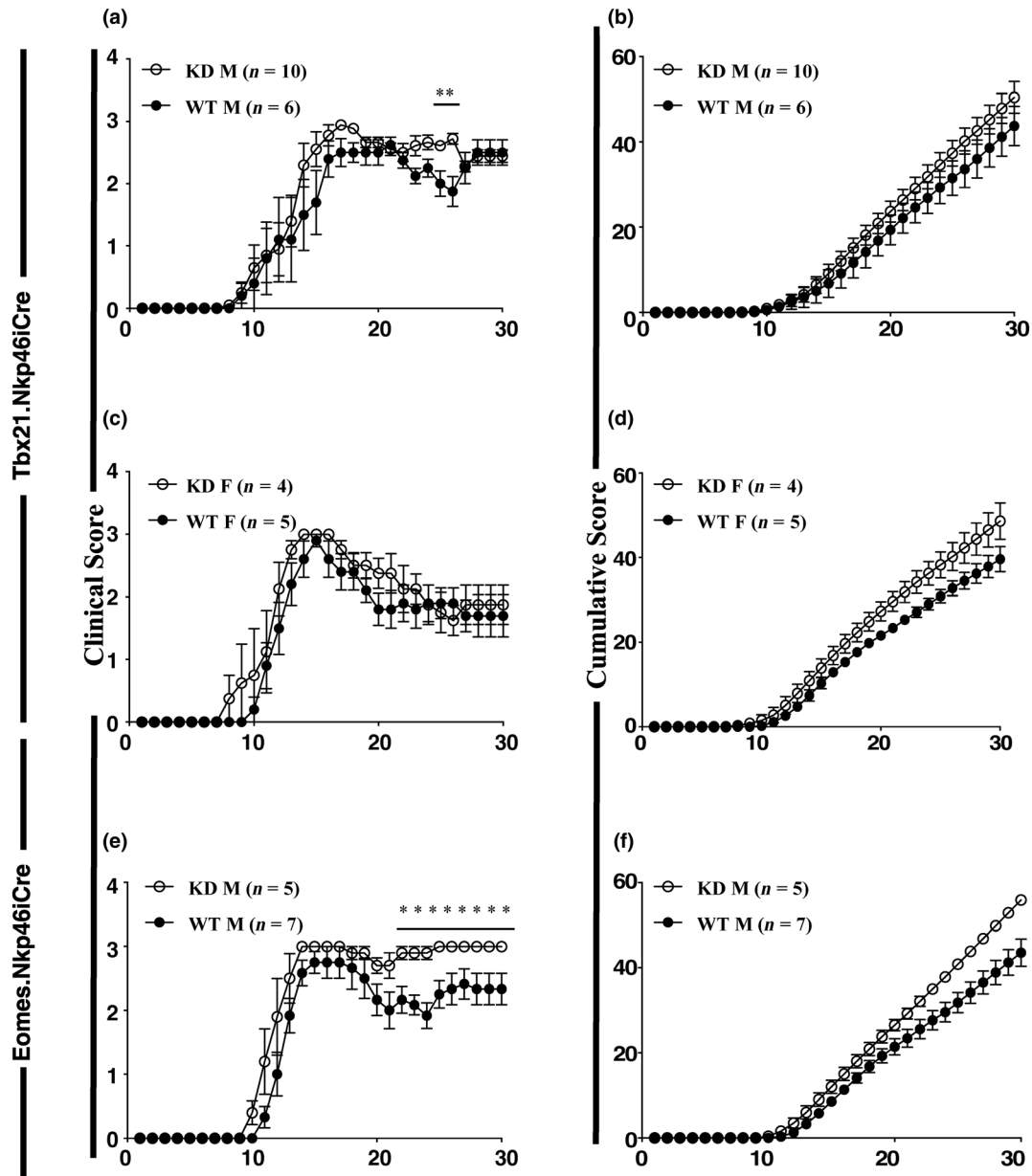
Figure 5. EAE following *in vivo* gene knockdown in NK cells. EAE disease course in **(a, b)** male and **(c, d)** female B6.*Tbx21.Nkp46iCre* + and B6.*Eomes.Nkp46iCre* + mice **(e, f)** (KD; open circles) compared with age-matched WT littermates (closed circles) from two independent experiments. There is no difference in the onset of EAE for either sex for either gene knockdown, but more severe disease without remit is observed for knockdown mice of both sexes **(b, d, f)**. Data are presented as mean $\pm$ standard error of the mean and each data point where there was a statistical difference in clinical score between the controls and KD mice is indicated by *. (Mann–Whitney *U*-test; $P < 0.05$, $n = 4$–10); EAE, MOG_{35-55}-induced experimental autoimmune encephalomyelitis; F, female; KD, gene knockdown mice; M, male; NK, natural killer; WT, wild type.

unable to reflect lineage-specific differences in transcription and may therefore have limited the types of interactions they described.

Overall, many studies on candidate gene functions suggest that networks of interactions are involved, rather than just individual "pathways", in contributing to the complex phenomena being studied. In addition, gene expression is cell type specific in time and space, and there remains a dispute over which immune cells are involved in initiating autoimmune attacks in MS. This prompted us to explore a WGCNA approach to identify associations between MS and gene expression. Our work

examines five purified peripheral blood leukocyte populations, sorted from peripheral blood mononuclear cells of 76 untreated patients with RRMS who are in remission and 104 HCs, making it one of the largest cohorts for gene expression studies of MS. Only patients with an MRI-confirmed RRMS diagnosis, where there had been no recent relapse, were included in the study. Measures to circumvent confounding gene expression changes were applied by collecting all peripheral blood samples in the early morning, at the same time of day, and ensuring no patient was administered any immunomodulatory therapeutic in the month before blood sampling. Control samples were from healthy individuals, unrelated to anyone with MS or with any other autoimmune disease.

We applied a WGCNA algorithm to batch-affect corrected microarray data (Combat R (http://biosun1.harvard.edu/complab/batch/) processed Affymetrix Human Gene 1.0 ST Arrays) of $CD4^+$ T cells, $CD8^+$ T cells, B cells, monocytes and NK cells from a mixed cohort of disease-affected and unaffected individuals. This resulted in the identification of 16 modules, consisting of 5762 transcripts, connected by 198 937 edges. Together, these represent 27.7% of all transcripts in the array. Differential expression analyses between RRMS and healthy individuals, for transcripts within each cell population, were mapped onto our transcriptional network and identified an integrated module of coexpressed genes (the BLACK module) associated with cytotoxicity in the monocytes, NK cells and CD8 T cells of patients with MS. Monocytes showed the greatest concentration of HDE transcripts (12 of 22 in the cell type) in any module across the entire experiment ($P < 10^{-34}$, χ^2 test), suggesting an important association with MS. More than this, of the 198 transcripts in the BLACK module, all but 11 were expressed on average at lower levels in monocytes of patients with MS than in those of HCs. Monocytes have a key role in myelin and axon destruction and auto-antigen presentation.[30] Active blood-borne monocytes have been found in abundance in MS lesions[31] together with activated T cells, macrophages and microglial cells,[30] while macrophages are restricted to the lesion perimeter in mixed active/inactive lesions[32] and are absent from inactive lesions. In addition, monocyte-derived proinflammatory and regulatory monokines remain active throughout disease progression and can be modulated by interferon-beta therapy.[33] Monocyte infiltration has also been associated with EAE progression,[34] and depleting them has been shown to reduce demyelination and ameliorate EAE.[35] It could, however, be argued that the algorithm used to construct the gene coexpression network was likely to favor this outcome, as it selected for transcripts that varied most in expression across all samples. However, strong negative correlations

between transcript expression levels are weighted equally with strong positive correlations when grouping into a single module. Furthermore, if the grouping was solely based on the happenstance of expression levels and did not reflect deeper coordination of functional coregulation, the members of the module would not have such a statistically strong bias to a shared functional role in immunobiology, namely, cell-mediated cytotoxicity.

We were able to partially replicate BLACK module downregulation seen in our patients in remission, both *in vitro* and *in vivo*, by targeting a small number of genes. By mimicking BLACK module downregulation in mice, the maximum severity of EAE was reduced, thereby suggesting that oppression of BLACK module expression in humans may contribute to MS induction/maintenance of remission, and that its downregulation is associated with reduced pathogenesis. How this module of cytotoxicity-related genes function in myeloid cells is presently unclear. Genes associated with classically activated *(Cxcl10)*, M1 *(TLR2, TLR4, CD68)*, M2a *(CD163)*, M2b *(CD163, CD86)* and M2c *(CD163)* macrophages as well as tumor-associated [*CD68, CD163*, C–C chemokine ligand 2 *(CCL2)*] macrophages were increased in our patient group compared with HCs, but whether the activation of any or all of them leads to macrophages taking on a cytotoxic function remains to be tested.

Therefore, while the WGCNA approach has provided a logistical framework that helps explain the association of MS with differential transcription of genes with a range of functions (suggesting the potential of multiple opportunities for intervention in the course of disease), the most likely explanation for the findings obtained in the studies of human blood leukocytes reported here is that they represent a hitherto unappreciated characteristic of the circulating monocytes of patients with RRMS in remission.

METHODS

Selection of patients and ethics statement

Healthy controls and pwRRMS who were currently in remission were recruited through the Box Hill Hospital and Royal Melbourne Hospital MS clinics. Participation in this study was voluntary and all samples were deidentified to ensure confidentiality and anonymity of the research respondents in compliance with the Eastern Health Research and Ethics Committee (E-080910) and Melbourne Health Human Research Ethics Committee (HREC/13/MH/189 2013.111) from whom ethics approvals were obtained. Criteria for inclusion in the patient cohort were (1) provision of informed consent; (2) a diagnosis of RRMS or clinically isolated syndrome suggestive of RRMS by McDonald criteria; (3) Expanded Disability Status Score recorded at the time of assessment; (4) no recent relapse and

(5) either untreated with a disease-modifying therapy or untreated for at least a month before venesection. This cohort overlapped significantly with patients used in our expression quantitative trait loci analyses.[12] Expanded Disability Status Score, sex, duration of disease and treatment were recorded. Venous blood (100 mL) was collected at a similar time of the day (between 9 am and 12 noon) and was transported on ice to the laboratory for immediate processing.

Processing of samples

Venous blood was separated into peripheral blood mononuclear cells, B cells, CD4$^+$ and CD8$^+$ T cells, NK cells and monocytes. In brief, peripheral blood mononuclear cells were isolated from 100 mL of venous blood using histopaque (Sigma-Aldrich, St Louis, MO) density gradient separation. The CD4$^+$ and CD8$^+$ T cells and CD19$^+$ B cells were purified by magnetic bead separation (positive selection) using Human Microbeads (Miltenyi Biotec, Macquarie Park, NSW, Australia) directed against the indicated cell surface markers as per the manufacturer's instructions using an autoMACS Pro (Miltenyi Biotec). The CD14$^+$ monocytes and NK (CD3$^-$ CD56$^+$) cells were first enriched using a STEMCELL Technologies' Monocyte or NK Enrichment Kit (STEMCELL Technologies, Tullamarine, Australia) as per the manufacturer's instructions, followed by positive selection with magnetic bead–bound anti-CD14 monoclonal antibody for monocyte selection, or anti-CD56 monoclonal antibody for NK cell selection using an autoMACS Pro. Following isolation, purity was assessed by FACS analysis of labeled antibodies CD4-PerCp (VIT4; Miltenyi Biotec), CD8-FITC (BW135/80; Miltenyi Biotec), CD20-PE (B lymphocytes; LT20; Miltenyi Biotec), CD14-PE (TUK4) and CD3-FITC (HIT3a; BD Pharmingen, Sparks, MD)/CD56-APC (AF12-7H3; Miltenyi Biotec) on a Cyan FACS Analyzer (Beckman Coulter, Inc., CA) to ensure highly enriched cell subsets were obtained with minimum contamination by other cells (Supplementary tables 1 and 2; Supplementary figure 1). Data were analyzed using WEASEL (version 3.0). Samples with purities below 95% were rejected for the comparison of expression between patients and controls of the individual subsets (average = 98.98% ± 0.06%). Samples were immediately suspended in RLT buffer of the Qiagen RNeasy kit (Qiagen, Venlo, Limburg, the Netherlands) and stored at –80°C until ready for extraction. A separate 3–10 mL aliquot of whole blood was also stored for DNA extraction.

RNA extraction and transcriptional analysis

Sorted leukocyte cell subsets were individually homogenized in the RLT buffer of an RNeasy kit (Qiagen, Limburg, the Netherlands); homogenates were passed through QIAshredder columns (Qiagen, Limburg, the Netherlands) and extracted as per manufacturer's instruction. The RNA yield was quantified spectrophotometrically on a Nanodrop ND-1000 (Thermo Fisher Scientific Inc., Wilmington, DE) and aliquots were electrophoresed for determination of sample concentration and purity. Following the manufacturer's recommendation, 100 ng

RNA/sample was used for labeling using the Affymetrix Whole Transcript (WT) Sense Target labelling Assay kit (Affymetrix, CA, USA). Labeled samples were hybridized to Affymetrix Human Gene_1.0 ST expression microarrays, that are designed to interrogate 28 869 well-annotated genes with 764 885 distinct 25-mer probes (median resolution of 26 probes/gene). Gene-level analysis of multiple probes on different exons were then summarised into an expression value representing all transcripts from the same gene. The probed arrays were washed and stained using the GeneChip Hybridization Wash and Stain Kit (Affymetrix, CA) and scanned using the GeneChip Scanner 3000. Images (.dat files) were processed using GeneChip Command Console (Affymetrix, CA) and CEL files were imported into Partek Genomics Suite 6.6 (Partek SG, Singapore) for further analysis.

Gene coexpression network construction and cell subset differential expression analyses of patients with MS and healthy controls

A gene coexpression network was constructed based on the expression values of 688 samples of purified peripheral blood leukocyte subsets from 76 pwRRMS and 104 HCs. This included a total of 442 HC samples and 246 patient samples, comprising the following subsets: B cells (89 HCs, 36 patients), CD4$^+$ T cells (85 HCs, 42 patients), CD8$^+$ T cells (72 HCs, 54 patients), monocytes (99 HCs, 57 patients), NK cells (90 HCs, 57 patients) and neutrophils (7 HC samples). The purpose of using leukocyte subsets, rather than mixed cell populations, was to empower the network to reflect lineage-specific differential expression, while the enrichment of the subject population with patients with MS was to enhance the likelihood of identifying MS-specific, cell-specific differences in transcript expression and their interactions within functional networked modules. The Affymetrix CEL files (Supplementary tables 3 and 4) were normalized using RMA background subtraction in Bioconductor and batch effects were removed using the nonparametric CombatR algorithm (http://biosun1.harvard.edu/complab/batch/)[36,37] as it has been demonstrated to result in better statistical power and control of false positives in differential expression compared with data adjusted by the other available methods, while successfully removing the batch effects and recovering the biological signal in the data.[37] A Pearson correlation of coexpression network construction was applied. Genes were ranked by standard deviations of the distribution of expression values across all patients and all cell types[16] and the data for the most variably expressed genes were used for network construction. A WGCNA algorithm in R[17] was applied to generate a weighted gene coexpression network (WGCN) and modules were colored in Cytoscape v3.10 (Institute of Systems Biology, Seattle, USA)[18] for ease of visualization. For each cell subset, significant *P*-values from the Students *t*-test comparison of expression of each gene in the network were mapped onto the network with a heat map to represent significance of difference in expression between patients and controls, as we have done previously for other analyses.[38]

Functional analysis of gene coexpression modules showing high differential expression between patients and controls

Module gene lists, identified as HDE between pwRRMS and HCs, were submitted to DAVID Bioinformatics Resources v6.7[19] for Gene Ontology analysis of functional annotation clustering against Clusters of Orthologous Groups (COG) Analysis Ontology, Sp Pir Keywords (SP-PIR), GO Biological Process (GO-BP), Molecular Function (GO-MF), Cellular Compartment (GO-CC), UniProt Sequence annotation (UP_SEQ_FEATURE), Online Mendelian Inheritance in Man (OMIM_DISEASE), Biological Biochemical Image Database (BBID), BioCarta Pathways (BIOCARTA) and Kyoto Encyclopedia of Genes and Genomes (KEGG). The repositories of curated biological interactions, Partek Pathways Software (Partek SG, Singapore) and Ingenuity Pathway Analysis (IPA, http://www.ingenuity.com), were also utilized for further exploration of the complex biological relationships and pathways and to assist in discovering meaningful biological insights and therapeutically relevant networks of significance.

siRNA transfection; RNA isolation and first-strand complementary DNA synthesis of THP-1 cells

Cells from monocyte tumor line, THP-1(ATCC#TI-B202), grown in complete Roswell Park Memorial Institute-1640 (RPMI-1640) medium without antibiotic (at a density of between 2×10^5 and 1×10^6 cells mL^{-1}) were incubated for 48 h (37°C; 5% CO_2; 95% humidity) in individual transfections with predesigned human Silencer Select siRNA (Thermo Fisher Scientific, Australia) targeting each candidate gene transcript—B4GALT6: s17835 (exon 2); BCL2L1: s1920 (exon 2); SYT11: s23284 (exon 2); TSPAN32: s19601 (exon 2); TTC38: s30006 (exon 7); OSBPL5: s377 (exon 21); STOM: s4716 (exon 7); PTPRA: s11534 (exon 9); TPST2: s16066 (exon 4); MLC1: s23287 (exon 10); NPC1: s9669 (exon 15); SYTL3: s41270 (exon 5); EOMES: s15832 (exon 6); TBX21: s26891 (exon 4); STAT4: s13531 (exon 10) or RUNX3: s2469 (exon 5)—together with Lipofectamine RNAiMAX Transfection reagent, as per supplier's instruction (Thermo Fisher Scientific). To increase transfection efficiency, THP-1 cells were passaged for at least 8 and not more than 30 generations and were grown in complete RPMI-1640 medium without antibiotic (at a density of 2×10^5 to 1×10^6 cells mL^{-1}) for at least 1 generation before siRNA transfection. BLOCK-iT Fluorescent Oligos (Thermo Fisher Scientific) were used as a positive control to estimate transfection efficiency, while untreated control wells contained Lipofectamine RNAiMAX alone. Transfection efficiency was determined by flow cytometry (BD LSRFortessa, Biosciences, NSW, Australia) as percentage of PE-high cells (successful endocytoses of BLOCK-iT Fluorescent Oligos) to total cells analyzed. No mycoplasma testing was undertaken. Harvested cells were washed in prewarmed phosphate-buffered saline and resuspended in 350 mL RLY Lysis Buffer (Bioline Reagents, UK) and 1% β-mercaptoethanol. RNA was extracted using the manufacturer's protocol of the ISOLATE II RNA Mini Kit

(Bioline Reagents, UK) and first-strand complementary DNA synthesized as per manufacturer's instruction of the TETRO cDNA synthesis kit (Bioline Reagents, UK). Because of the relatively low RNA yield isolated from siRNA-treated samples, 12 μL of total RNA was used in each real-time PCR. Complementary DNA was stored at −20°C until further use.

Real-time PCR

Primers specific for target genes' transcript, off-target transcript and house-keeping control were designed according to standard PCR primer design parameters using the PRIMER-BLAST online tool available on the National Center for Biotechnology Information (NCBI) website (www.ncbi.nlm.nih.gov), with preference for at least one primer to span an exon–exon junction, producing a single amplicon product size in the range of 50–200 bp and melting temperature of 60°C. Primer sequences are available in Supplementary table 5.

Real-time PCR was performed on Rotor-Gene 6000 (Qiagen, Limburg, the Netherlands), using the SensiFAST SYBR No-ROX kit (Bioline Reagents, UK) according to the manufacturer's protocol. In brief, for every 15 μL reaction, 7.5 μL of SensiFAST SYBR No-ROX Master Mix was mixed with 0.3 μL of each forward and reverse 10 μM primer, 1 μL of complementary DNA and nuclease-free water. Real-time PCR was performed with an initial denaturation step at 94°C for 2 min, followed by 40 cycles of 94°C for 20 s (denaturation) and 60°C for 30 s (annealing and elongation). Amplification specificity was confirmed via melting curve analysis with a temperature gradient (60–95°C; 0.5°C increment/10 s). Gene expression was measured using the Pfaffl mathematical method of relative quantitative real-time PCR (Pfaffl[39]). Ct values of siRNA-treated samples and untreated control for each gene were obtained using the same reaction mixture and quantitative PCR settings. All independent quantitative PCRs were performed in duplicate to obtain an averaged Ct value. Expression of individual genes in the siRNA-treated sample *versus* the control, normalized to *GAPDH* as the reference gene, was expressed as fold change. Negative inverse $(-1/x)$ was used for ratio values that were less than 1 (e.g. a ratio of 0.5 was converted to −2-fold-change). All results are presented as average fold change, and no change in expression as "1".

Mice and EAE induction

Conditional knockout-ready mice for *Eomes* [B6.129S1(Cg)-Eomes$^{tm1.1Bflu}$/J, Stock # 017293] and *Tbx21* (B6.129-Tbx21^{tm2Srnr}/J, Stock #022741) were obtained from The Jackson Laboratory as homozygous mutants, which we backcrossed for three generations to C57BL/6J mice in our facility, before intercrossing to maintain them as homozygous conditional-ready mice for experimental use. Floxed mice were identified by genotyping using primers:

- Eomes F 5′-AGA TGG AAA TTT GGG AAT GAA-3′,
- Eomes R 5′-GGC TAC TAC GGC CTG AAA CT-3′,
- Tbx21 F 5′-AGT CCC CCT GGA AGA ACA CT-3′,
- Tbx21 R 5′-TGA AGG ACA GGA ATG GGA AC-3′.

To target KD to the myeloid cell lineage including monocytes, mature macrophages and granulocytes, floxed mice were crossed to C57BL/6.LysMCre mice (http//jaxmice.jax.org, strain # 004781), in which the *LysMCre* knock-in allele has a nuclear-localized Cre recombinase inserted into the first-coding ATG of the lysosome 2 gene (*Lyz2*), both abolishing endogenous *Lyz2* gene function and placing NLS-*Cre* expression under the control of the endogenous *Lyz2* promoter/enhancer element.[40] Male or female mice carrying both the *Cre* and the floxed allele were then bred with heterozygous-floxed (*Eomes* or *Tbx21*) mice or otherwise were intercrossed, and floxed-heterozygous littermates, Cre$^+$ and Cre$^-$, were selected by genotyping, for experimentation. The lack of allele recombination was confirmed by PCR using primers:

- IMR3066 KI R 5′-CCC AGA AAT GCC AGA TTA CG-3′,
- IMR3067 F 5′-CTT GGG CTG CCA GAA TTT CTC-3′,
- IMR3068 WT R 5′-TTA CAG TCG GCC AGG CTG AC-3′.

Mutant allele ~700 bp; WT 350 bp (homozygous mutants may give fragment ~1500–2000 bp for WT allele).

To generate mice with targeted KD in NK cells, *Eomes* or *Tbx21* floxed mice were crossed with C57BL/6.Nkp46iCre mice [C57BL/6-Ncr1$^{tm1.1(icre)Viv}$/Orl, Eric Vivier, International Mouse Strain Resource[41]], in which *Cre* recombinase expression was under the control of *Ncr1* (also called *Nkp46*) gene promoter. Male or female mice carrying both the *Cre* and the floxed allele were then bred with heterozygous-floxed (*Eomes* or *Tbx21*) mice or otherwise were intercrossed, and floxed-heterozygous littermates, Cre$^+$ and Cre$^-$ were selected by genotyping, for experimentation. The lack of allele recombination was confirmed by PCR using primers to distinguish all three potential alleles (modified allele ~247 bp, WT allele 300 bp):

- Nkp46iCre F 5′-GGA ACT GAA GGC AAC TCC TG-3′,
- Nkp46iCre KI R 5′-CCC TAG GAA TGC TCG TCA AG-3′,
- Nkp46iCre WT R 5′-TTC CCG GCA ACA TAA AAT AAA-3′.

Active EAE was induced in 8–12-week-old mice by injection of 200 μL MOG$_{35-55}$/phosphate-buffered saline: CFA (1:1) [200 mg MOG$_{35-55}$ peptide (Auspep, Parkville, VIC, Australia)] in 100 mL phosphate-buffered saline emulsified in an equal volume (1:1) of IFA (Sigma-Aldrich, Castle Hill, NSW, Australia) containing 0.5 mg heat-killed *M. tuberculosis* H37RA (DIFCO; BD Diagnostic Systems, Sparks, MD) at day 0 between the shoulder blades. The mice also received intraperitoneal injection of 250 ng PTX (List Biological Laboratories, Campbell, CA) at the day of immunization and 2 days later. Disease progression was scored daily from day 8 after initial injection, for 30 days.[42] Clinical symptoms of EAE were scored as follows: 0, no symptoms; 0.5, tail weakness or partial tail paralysis; 1, total tail paralysis; 1.5, weakened hind limb; 2, partial hind limb paralysis, unbalanced movement; 2.5 total paralysis of a hind limb; 3, total hind limbs paralysis; 3.5 weakened forelimb, difficulty in reaching for food; 4, all limbs paralyzed and 5, moribund or dead. Soft food and DietGel Recovery nutrient gel (ClearH2O) were provided when mice reached a score of 2 or higher. Mice that reached a score of 3.5 or higher were killed, because of their restricted movement compromising their access to food and water. Mice that had lost at least 20% of their body weight (as measured from day 0) for 3 consecutive days were killed in accordance with the animal ethics guideline. At the end of the experiments, mice were killed by CO$_2$ asphyxiation and disposed of by deep burial. These studies have been reviewed and approved by the James Cook University Animal Ethics Committee (A1894, AA2621, A2821). The study was carried out in compliance with the Animal Research: Reporting of In Vivo Experiments (ARRIVE) guidelines (https://arriveguidelines.org) and all methods were performed in accordance with the relevant guidelines and regulations.

Statistical analyses

Qualitative data were compared by Fisher's exact test or contingency table (chi-squared) analysis and quantitative data by analysis of variance, *t*-tests and Mann–Whitney *U*-tests as calculated by GraphPad Prism 9 (La Jolla, CA).

AUTHOR CONTRIBUTIONS

CONFLICT OF INTEREST

DATA AVAILABILITY STATEMENT

The CEL files for gene expression have been deposited at the European Genome-phenome Archive (EGA), which is hosted by the European Bioinformatics Institute (EBI) and the Centre for Genomic Regulation (CRG), under accession number EGAS00001007452, with some CEL files overlapping with our previous publication,[12] accessible under accession number EGAS00001004087. Further information about EGA can be found at https://ega-archive.org "The European Genome-phenome Archive of human data consented for biomedical research" http://www.nature.com/ng/journal/v47/n7/full/ng.3312.html.

REFERENCES

1. Simpson S, Pittas F, Van Der Mei I, Blizzard L, Ponsonby A-L, Taylor B. Trends in the epidemiology of multiple sclerosis in greater Hobart, Tasmania: 1951 to 2009. *J Neurol Neurosurg Psychiatry* 2011; **82**: 180–187.

2. Jordan MA, Field J, Butzkueven H, Baxter AG. Genetic predisposition, humans. The Autoimmune Diseases. Amsterdam: Elsevier; 2014:341–364.

3. Jordan MA, Baxter AG. Genetic predisposition, humans. The Autoimmune Diseases. Amsterdam: Elsevier; 2020:383–418.

4. Hammond S, McLeod J, Millingen K, *et al*. The epidemiology of multiple sclerosis in three Australian cities: Perth, Newcastle and Hobart. *Brain* 1988; **111**: 1–25.

5. Beecham AH, Patsopoulos NA, Xifara DK, *et al*. Analysis of immune-related loci identifies 48 new susceptibility variants for multiple sclerosis. *Nat Genet* 2013; **45**: 1353–1360.

6. Fagnani C, Neale MC, Nisticò L, *et al*. Twin studies in multiple sclerosis: a meta-estimation of heritability and environmentality. *Mult Scler* 2015; **21**: 1404–1413.

7. Westerlind H, Ramanujam R, Uvehag D, *et al*. Modest familial risks for multiple sclerosis: a registry-based study of the population of Sweden. *Brain* 2014; **137**: 770–778.

8. Consortium IMSG, ANZgene, IIBDGC, WTCCC2. Multiple sclerosis genomic map implicates peripheral immune cells and microglia in susceptibility. *Science* 2019; **365**: eaav7188.

9. Bahlo M, Booth DR, Broadley S, *et al*. Genome-wide association study identifies new multiple sclerosis susceptibility loci on chromosomes 12 and 20. *Nat Genet* 2009; **41**: 824–828.

10. Consortium IMSG. Risk alleles for multiple sclerosis identified by a genomewide study. *N Engl J Med* 2007; **357**: 851–862.

11. Consortium IMSG, WTCCC2, Sawcer S, Hellenthal G, Pirinen M, *et al*. Genetic risk and a primary role for cell-mediated immune mechanisms in multiple sclerosis. *Nature* 2011; **476**: 214–219.

12. Gresle MM, Jordan MA, Stankovich J, *et al*. Multiple sclerosis risk variants regulate gene expression in innate and adaptive immune cells. *Life Sci Alliance* 2020; **3**: e202000650.

13. Barabasi A-L, Oltvai ZN. Network biology: understanding the cell's functional organization. *Nat Rev Genet* 2004; **5**: 101–113.

14. Stuart JM, Segal E, Koller D, Kim SK. A gene-coexpression network for global discovery of conserved genetic modules. *Science* 2003; **302**: 249–255.

15. Zhou X, Kao M-CJ, Wong WH. Transitive functional annotation by shortest-path analysis of gene expression data. *Proc Natl Acad Sci USA* 2002; **99**: 12783–12788.

14401711, 0, Downloaded from https://onlinelibrary.wiley.com/doi/10.1111/imcb.12793 by Eddie Koiki Mabo Library, Wiley Online Library on [25/06/2024]. See the Terms and Conditions (https://onlinelibrary.wiley.com/terms-and-conditions) on Wiley Online Library for rules of use; OA articles are governed by the applicable Creative Commons License

16. Hahne F, Mehrle A, Arlt D, Poustka A, Wiermann S, Beissbarth T. Extending pathways based on gene lists using InterPro domain signatures. *BMC Bioinform* 2008; **9**: 3.

17. Langfelder P, Horvath S. WGCNA: an R package for weighted correlation network analysis. *BMC Bioinform* 2008; **9**: 559.

18. Shannon P, Markiel A, Ozier O, *et al.* Cytoscape: a software environment for integrated models of biomolecular interaction networks. *Genome Res* 2003; **13**: 2498–2504.

19. Huang DW, Sherman BT, Lempicki RA. Systematic and integrative analysis of large gene lists using DAVID bioinformatics resources. *Nat Protoc* 2009; **4**: 44–57.

20. Lazarevic V, Glimcher LH, Lord GM. T-bet: a bridge between innate and adaptive immunity. *Nat Rev Immunol* 2013; **13**: 777–789.

21. Gordon SM, Chaix J, Rupp LJ, *et al.* The transcription factors T-bet and Eomes control key checkpoints of natural killer cell maturation. *Immunity* 2012; **36**: 55–67.

22. Parnell GP, Gatt PN, Krupa M, *et al.* The autoimmune disease-associated transcription factors EOMES and TBX21 are dysregulated in multiple sclerosis and define a molecular subtype of disease. *Clin Immunol* 2014; **151**: 16–24.

23. McKay FC, Gatt PN, Fewings N, *et al.* The low EOMES/TBX21 molecular phenotype in multiple sclerosis reflects CD56$^+$ cell dysregulation and is affected by immunomodulatory therapies. *Clin Immunol* 2016; **163**: 96–107.

24. Nickles D, Chen HP, Li MM, *et al.* Blood RNA profiling in a large cohort of multiple sclerosis patients and healthy controls. *Hum Mol Genet* 2013; **22**: 4194–4205.

25. Menon R, Di Dario M, Cordiglieri C, *et al.* Gender-based blood transcriptomes and interactomes in multiple sclerosis: involvement of SP1 dependent gene transcription. *J Autoimmun* 2012; **38**: J144–J155.

26. Krämer A, Green J, Pollard J Jr, Tugendreich S. Causal analysis approaches in ingenuity pathway analysis. *Bioinformatics* 2014; **30**: 523–530.

27. Palacios R, Goni J, Martinez-Forero I, *et al.* A network analysis of the human T-cell activation gene network identifies JAGGED1 as a therapeutic target for autoimmune diseases. *PLoS One* 2007; **2**: e1222.

28. Riveros C, Mellor D, Gandhi KS, *et al.* A transcription factor map as revealed by a genome-wide gene expression analysis of whole-blood mRNA transcriptome in multiple sclerosis. *PLoS One* 2010; **5**: e14176.

29. Creanza TM, Liguori M, Liuni S, Nuzziello N, Ancona N. Meta-analysis of differential connectivity in gene Co-expression networks in multiple sclerosis. *Int J Mol Sci* 2016; **17**: 936.

30. Frischer JM, Bramow S, Dal-Bianco A, *et al.* The relation between inflammation and neurodegeneration in multiple sclerosis brains. *Brain* 2009; **132**: 1175–1189.

31. Kouwenhoven MCM, Teleshova N, Özenci V, Press R, Link H. Monocytes in multiple sclerosis: phenotype and cytokine profile. *J Neuroimmunol* 2001; **112**: 197–205.

32. Kuhlmann T, Ludwin S, Prat A, Antel J, Brück W, Lassmann H. An updated histological classification system for multiple sclerosis lesions. *Acta Neuropathol* 2017; **133**: 13–24.

33. Filion LG, Graziani-Bowering G, Matusevicius D, Freedman MS. Monocyte-derived cytokines in multiple sclerosis. *Clin Exp Immunol* 2003; **131**: 324–334.

34. Ajami B, Bennett JL, Krieger C, McNagny KM, Rossi F. Infiltrating monocytes trigger EAE progression, but do not contribute to the resident microglia pool. *Nat Neurosci* 2011; **14**: 1142–1149.

35. Bhasin M, Wu M, Tsirka SE. Modulation of microglial/macrophage activation by macrophage inhibitory factor (TKP) or tuftsin (TKPR) attenuates the disease course of experimental autoimmune encephalomyelitis. *BMC Immunol* 2007; **8**: 10.

36. Johnson WE, Li C, Rabinovic A. Adjusting batch effects in microarray expression data using empirical Bayes methods. *Biostatistics* 2007; **8**: 118–127.

37. Zhang Y, Parmigiani G, Johnson WE. ComBat-seq: batch effect adjustment for RNA-seq count data. *NAR Genom Bioinform* 2020; **2**: lqaa078.

38. Dinh XT, Stanley D, Smith LD, *et al.* Modulation of TCR signalling components occurs prior to positive selection and lineage commitment in iNKT cells. *Sci Rep* 2021; **11**: 23650.

39. Pfaffl MW. A new mathematical model for relative quantificationin real-time RT-PCR. *Nucleic Acids Res* 2001; **29**: e45.

40. Clausen BE, Burkhardt C, Reith W, Renkawitz R, Forster I. Conditional gene targeting in macrophages and granulocytes using LysMcre mice. *Transgenic Res* 1999; **8**: 265–277.

41. Narni-Mancinelli E, Chaix J, Fenis A, *et al.* Fate mapping analysis of lymphoid cells expressing the NKp46 cell surface receptor. *Proc Natl Acad Sci USA* 2011; **108**: 18324–18329.

42. Miranda-Hernandez S, Gerlach N, Fletcher JM, *et al.* Role for MyD88, TLR2 and TLR9 but not TLR1, TLR4 or TLR6 in experimental autoimmune encephalomyelitis. *J Immunol* 2011; **187**: 791–804.

SUPPORTING INFORMATION

Additional supporting information may be found online in the Supporting Information section at the end of the article.